

## NON-LTE EFFECTS ON THE $H_3^+$ ROVIBRATIONAL POPULATION IN THE JOVIAN IONOSPHERE

YONG HA KIM

Department of Astronomy and Space Science, Chungnam National University, Daejeon 305-764, Korea

*E-mail:* yhkim@cnu.ac.kr

(Received January 03, 2012; Revised February 10, 2012; Accepted February 26, 2012)

### ABSTRACT

We investigate non-LTE effects on the  $H_3^+$  level populations to help the analysis of the observed 2 and 3.5 micron  $H_3^+$  emissions from the Jovian ionosphere. We begin by constructing a simple three-level model, in order to compute the intensity ratio of the R(3,4) line in the hot band to the Q(1,0) line in the fundamental band, which have been observed in the Jovian auroral regions. We find that non-LTE effects produce only small changes in the intensity ratios for ambient  $H_2$  densities less than or equal to  $5 \times 10^{11} \text{ cm}^{-3}$ . We then construct two comprehensive models by including all the collisional and radiative transitions between pairs of more than a thousand known  $H_3^+$  rovibrational levels with energies less than  $10000 \text{ cm}^{-1}$ . By employing these models, we find that the intensity ratios of the lines in the hot and fundamental bands are affected greatly by non-LTE effects, but the details depend sensitively on the number of collisional and radiative transitions included in the models. Non-LTE effects on the rovibrational population become evident at about the same ambient  $H_2$  densities in the comprehensive models as in the three-level model. However, the models show that rotational temperatures derived from the intensities of rotational lines in the  $\nu_2$  and  $2\nu_2$  bands may differ significantly from the ambient temperatures in the non-LTE regime. We find that significant non-LTE effects appear near and above the  $H_3^+$  peak, and that the kinetic temperatures in the Jovian thermospheric temperatures derived from the observed line ratios in the 2 and 3.5 micron  $H_3^+$  emissions are highly model dependent.

*Key words* : Planets: Jupiter — Ionosphere: Modeling

### 1. INTRODUCTION

$H_3^+$  emissions were observed for the first time outside the laboratory from the Jovian auroral regions in the 2 micron overtone ( $\nu_2 = 2 - 0$ ) bands (Drossart et al. 1989). Since that study, the intensities of lines in the fundamental ( $\nu_2 = 1 - 0$ ) and hot ( $\nu_2 = 2 - 1$ ) bands in 3.5 micron wavelength regions, as well as those in the 2 micron hot overtone ( $\nu_2 = 3 - 1$ ) and overtone bands ( $\nu_2 = 2 - 0$ ), have been measured in numerous spectra of the Jovian ionosphere (e.g., Maillard et al. 1990; Miller et al. 1997; Stallard et al. 2002; Raynaud et al. 2004). The total  $H_3^+$  column densities and column averaged temperatures have been deduced from the observed line emissions by considering the vibrational populations to be in quasi-local thermodynamic equilibrium (quasi-LTE) with the background thermosphere (e.g., Lam et al. 1997). Because infrared emission of  $H_3^+$  is the most important cooling process in the thermospheres of the Jovian planets, an accurate determination of the  $H_3^+$  column densities and the infrared emission intensities is essential.

It has been suggested that non-LTE effects may be significant in determining the populations of the vibrational levels of  $H_3^+$  in the Jovian ionosphere. A model for the relative populations of the vibrational levels

showed significant depopulations of  $\nu_2 = 1$  and 2 by fast radiative relaxation (Kim et al. 1992). Stallard et al. (2002) developed a simple three level model to account for the observed intensity ratios of lines in the fundamental band to those in the hot band. This model predicted higher temperatures at  $H_3^+$  emission altitudes than those usually proposed for the auroral/polar regions by several hundred Kelvins (Grodent et al. 2001). Recently, Melin et al. (2005) predicted large departures of the  $H_3^+$  populations from LTE in the region above 800 km (referred to the 1 bar level) in the Jovian ionosphere.

In this paper, we investigate non-LTE effects on the Jovian  $H_3^+$  emissions in two ways. Firstly, we assess the reliability of the simple three-level model in accounting for the observed intensity ratios of lines in the fundamental and hot bands. Secondly, we develop a more complex model which includes all the known rovibrational levels of  $H_3^+$  up to energies of  $10000 \text{ cm}^{-1}$ , and the transitions between pairs of levels. We then use this model to compute the relative rovibrational populations for the conditions in the Jovian ionosphere. All previous models have included either only the vibrational states or a few rovibrational levels surrogate to vibrational states, but not the individual rovibrational levels in vibrational states. We utilize an exten-

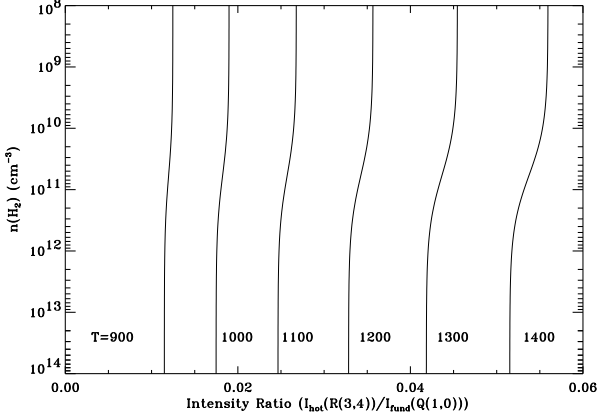


**Fig. 1.**— Intensity ratio of the line R(3,4) in the hot band to the line Q(1,0) in the fundamental band vs. ambient  $\text{H}_2$  densities at various temperatures for the simple three-level model. See the main text for details.

sive critical compilation of  $\text{H}_3^+$  rovibrational levels and transitions, which was taken from laboratory data over the past two decades by Lindsay and McCall (2001) (hereafter LM2001). In order to estimate the sensitivity of the model to the input data, we have also constructed an alternative model which uses the compilation of the energies and transition probabilities between the rovibrational levels of  $\text{H}_3^+$  determined by the theoretical calculations of Neale et al. (1996) (hereafter UCL1996).

## 2. A THREE-LEVEL POPULATION MODEL OF $\text{H}_3^+$

Simple three level models have been used to estimate thermospheric temperatures from the observed intensities of the 2 and 3.5 micron  $\text{H}_3^+$  lines in the Jovian aurora by Miller et al. (1997) and Stallard et al. (2002). Following Stallard et al., we construct a similar three level model for the R(3,4) line in the hot band and the Q(1,0) line in the fundamental band, which takes into account collisional excitation and deexcitation between the ground level ( $v_2 = 0$ ) and two upper levels - i.e., ( $v_2 = 2, J = 4, G = 4$ ) and ( $v_2 = 1, J = 1, G = 0$ ); and radiative decay from the two upper levels to the ground state. Under steady state conditions, the production and loss rates of both the upper levels of  $\text{H}_3^+$  are equal. These equalities can be expressed by the following equations:

$$n_0 n(\text{H}_2) k_{02} = n_2 (n(\text{H}_2) k_{20} + \Sigma_k A_{2k}) \quad (1)$$

$$n_0 n(\text{H}_2) k_{01} = n_1 (n(\text{H}_2) k_{10} + \Sigma_k A_{1k}) \quad (2)$$

where  $k_{i,j}$  is the rate coefficient for collisional excitation or deexcitation from level  $i$  to level  $j$ ; the ground, first, and second levels are here designated by the subscripts  $i$  or  $j$  equal to 0, 1, and 2, respectively;  $n_i$  is the number density of the level  $i$  of  $\text{H}_3^+$ ;  $A_{ji}$  is the transition probability for radiative decay from an upper level

$j$  to a lower level  $i$ . Therefore,  $n(\text{H}_2)k_{ij}$  represents the collision frequency for transitions from level  $i$  to level  $j$  of  $\text{H}_3^+$  by collisions with  $\text{H}_2$ . Also the relationship between the rate coefficients for collisional excitation,  $k_{ij}$ , and deexcitation,  $k_{ji}$ , is given by the principle of detailed balance as

$$k_{ij} = k_{ji} (g_j/g_i) \exp(-E_{ji}/kT), \quad (3)$$

where  $g_i$  is the statistical weight of level  $i$  and  $E_{ji} = E_j - E_i$  is the energy difference between the  $j$  and  $i$  levels. Deexcitation is assumed to occur by collisions of  $\text{H}_3^+$  with thermospheric  $\text{H}_2$ , with a temperature independent rate coefficient  $k_{10} = k_{20} = 2 \times 10^{-9} \text{ cm}^3 \text{ s}^{-1}$ , which is approximately the Langevin value,  $k_c$ . Stallard et al. (2002) assumed a temperature dependent deexcitation rate coefficient of  $10^{-9} (T/1000)^{0.5} \text{ cm}^3 \text{ s}^{-1}$  in their three-level model. Reactions between a non-polar neutral species and an ion at low velocities are given to first order by polarization theory, in which the cross section is proportional to  $v^{-1}$ , where  $v$  is the relative velocity. Therefore, the rate coefficient  $k_c = \langle v\sigma(v) \rangle$ , which represents an average of  $v\sigma(v)$  over the relative velocity distribution (usually a Maxwell-Boltzmann distribution), is independent of temperature. The Langevin (or gas kinetic) rate coefficient for the reaction of  $\text{H}_3^+ + \text{H}_2$  for pure polarization theory is  $\sim 1.9 \times 10^{-9} \text{ cm}^3 \text{ s}^{-1}$ .

The number density ratio of  $\text{H}_3^+$  level 2 to level 1 can be derived as

$$n_2/n_1 = g_2/g_1 \exp(-E_{21}/kT) \times \frac{1 + \Sigma A_{1k}/n(\text{H}_2)k_{10}}{1 + \Sigma A_{2k}/n(\text{H}_2)k_{20}}. \quad (4)$$

If the collisional de-excitation frequencies,  $n(\text{H}_2)k_{10}$  and  $n(\text{H}_2)k_{20}$  are substituted by the inverse of the collisional lifetime  $\tau_c \equiv n(\text{H}_2)k_c$ , the intensity ratio of R(3,4) to Q(1,0) can then be expressed as

$$I_{hot}(R)/I_{fund}(Q) = \frac{n_2 A_{21}(R) h\nu_{21}}{n_1 A_{10}(Q) h\nu_{10}} = \frac{g_2 E_{21}}{g_1 E_{10}} \times \exp(-E_{21}/kT) \frac{\tau_c (\Sigma A_{1k})/A_{10}(Q) + 1/A_{10}(Q)}{\tau_c (\Sigma A_{2k})/A_{21}(R) + 1/A_{21}(R)} \quad (5)$$

where  $A_{10}(Q)$  and  $A_{21}(R)$  are the transition probabilities of the Q and R branches, that is, from the levels ( $v_2 = 1, J = 1, G = 0$ ) and ( $v_2 = 2, J = 4, G = 4$ ) to ( $v_2 = 0, J = 1, G = 0$ ) and ( $v_2 = 0, J = 3, G = 4$ ), respectively. The quantities  $\Sigma A_{1k}$  and  $\Sigma A_{2k}$  are sums of all the transition probabilities from the levels ( $v_2 = 1, J = 1, G = 0$ ) and ( $v_2 = 2, J = 4, G = 4$ ) to possible lower levels, respectively.

Note that the intensity ratio differs from that shown in Eq. 9 of Stallard et al. (2002), in which there is an inverse of the factor  $\exp(-E/kT)$  after  $\tau_c$ . This factor has already been accounted for when the collisional

excitation rate coefficients were related to the deexcitation rate coefficients by the principle of detailed balance.

Using the same values for the constants in Eq. 5 as given in Table 1 of Stallard et al. (2002), we have computed the intensity ratios as a function of temperature  $T$  and H<sub>2</sub> number densities  $n(\text{H}_2)$ . The results are shown in Fig. 1. The intensity ratios of the lines in the hot bands to those in the fundamental bands vary only weakly as a function of the ambient H<sub>2</sub> densities, with only about an 8% increase from H<sub>2</sub> densities of  $10^{14}$  to  $10^8 \text{ cm}^{-3}$ . Therefore, this simple non-LTE analysis shows that the particular line ratio is not a good indicator of the ambient H<sub>2</sub> densities at H<sub>3</sub><sup>+</sup> emission altitudes, which was hoped to be estimated from observations of the Jovian auroral H<sub>3</sub><sup>+</sup> emission by Stallard et al. (2002).

At high neutral densities, where  $\tau_c \rightarrow 0$  and LTE prevails, the line ratio is close to that of the Einstein A coefficients times the thermal population ratio,  $n_2/n_1$ ,

$$I_{hot}(R)/I_{fund}(Q) \approx g_2/g_1 \exp(-E_{21}/kT) \times A_{21}(R)/A_{10}(Q). \quad (6)$$

In the limit of low densities, where  $\tau_c \rightarrow \infty$  (the non-LTE region), the line ratio approaches the ratio of the branching fractions times the thermal population;

$$I_{hot}(R)/I_{fund}(Q) \approx g_2/g_1 \exp(-E_{21}/kT) \times (A_{21}(R)/\sum A_{2k})/(A_{10}(Q)/\sum A_{1k}). \quad (7)$$

The line ratio thus increases as the H<sub>2</sub> density decreases, because the ratio of the Einstein A coefficients for these particular lines,  $A_{21}(R)/A_{10}(Q) = 66/129$ , is smaller than the ratio of branching fractions,  $(A_{21}(R)/\sum A_{2k})/(A_{10}(Q)/\sum A_{1k}) = (1/1.8)/1$ , where  $\sum A_{2k}$  and  $\sum A_{1k}$  are sums over all possible radiative decays from the top and second levels, respectively. The top level ( $v_2 = 2, J = 4, G = 4$ ) can radiate into the level ( $v_2 = 1, J = 5, G = 4$ ) (P-branch) and the level ( $v_2 = 1, J = 4, G = 4$ ) (Q-branch), as well as into the level ( $v_2 = 2, J = 3, G = 4$ ), which gives the R-branch transition of interest here. However, the second level ( $v_2 = 1, J = 1, G = 0$ ) can only radiatively decay to the level ( $v_2 = 0, J = 1, G = 0$ ) via Q-branch. Other transitions from the second level are not allowed. The radiative transition strengths are adopted from Neal et al (1996), as done in Stallard et al (2002). The model of Stallard et al. (2002) also shows non-LTE effects, but opposite to the model presented here.

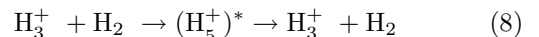
Fig. 1 shows that non-LTE effects on the line ratios begin to appear at H<sub>2</sub> densities of  $10^{12} \text{ cm}^{-3}$  or less, which correspond to the region above the peak of the Jovian auroral H<sub>3</sub><sup>+</sup> density profile (Grodent et al. 2001; Perry et al. 1999). In this model, the critical H<sub>2</sub> density for the onset of non-LTE can be estimated by equating the collisional lifetime to the radiative lifetime  $\tau_r$ , i.e.,  $\tau_c = \tau_r = A_{ji}^{-1}$ . The simple three level model,

however, ignores many transitions to and from other rovibrational levels of H<sub>3</sub><sup>+</sup>, and the levels chosen may not be representative of other levels in the vibrational manifolds. Thus the construction of a comprehensive model that includes many more collisional and radiative transitions between as many rovibrational levels as possible is desirable.

### 3. A ROVIBRATIONAL POPULATION MODEL OF H<sub>3</sub><sup>+</sup>

LM2001 have published a critical compilation of the lines in the H<sub>3</sub><sup>+</sup> spectrum. A total of 1012 rovibrational levels with energies up to  $10000 \text{ cm}^{-1}$  are included in this study, based on a comparison of measured transitions with recent theoretical calculations. The identification of the levels is complete for those with energies up to  $9000 \text{ cm}^{-1}$ . A total of 823 radiative transitions is identified in LM2001 between pairs of 895 levels reported by laboratory studies since 1980. In their theoretical approach, UCL1996 have calculated Einstein A factors for more than 3 million transitions between rovibrational levels with energies below  $15,000 \text{ cm}^{-1}$ . These data are available from the University College London (UCL) website (<http://www.tampa.phys.ucl.ac.uk/ftp/astrodata/h3+>). In order to test the sensitivity of the model outlined here with respect to the details of the transitions, we have constructed two models in which the LM2001 and the UCL1996 line lists are adopted for energy levels up to  $10000 \text{ cm}^{-1}$ .

Collisional excitation and de-excitation are important in determining the level populations, but the individual rate coefficients have not been measured nor calculated. Collisions with ambient H<sub>2</sub> are critical in determining the H<sub>3</sub><sup>+</sup> vibrational levels, since the Jovian thermosphere consists of mainly H<sub>2</sub>. The reactions apparently proceeds via an intermediate (H<sub>5</sub><sup>+</sup>)<sup>\*</sup>, which can be expressed as:



in which the (H<sub>5</sub><sup>+</sup>)<sup>\*</sup> intermediate survives for several rotational periods. Consequently, the identities of the five protons are interchanged, and the final rovibrational levels of H<sub>3</sub><sup>+</sup> are populated nearly randomly, constrained only by energy conservation. Based on the assumption of complete randomness of the collision process, we estimate the collisional de-excitation coefficients,  $k_{ji}$ , from the upper level  $j$  to lower level  $i$ , to be proportional to the statistical weight  $g_i$  of the lower level. We normalize the sum of de-excitation coefficients to all the levels lower than  $j$  to be equal to the Langevin rate coefficient,  $2 \times 10^{-9} \text{ cm}^3 \text{ s}^{-1}$ . The collisional excitation coefficients are computed from the corresponding de-excitation coefficients using the principle of detailed balance. Note that the individual de-excitation coefficients are smaller for higher levels than for lower levels, because high levels have more lower

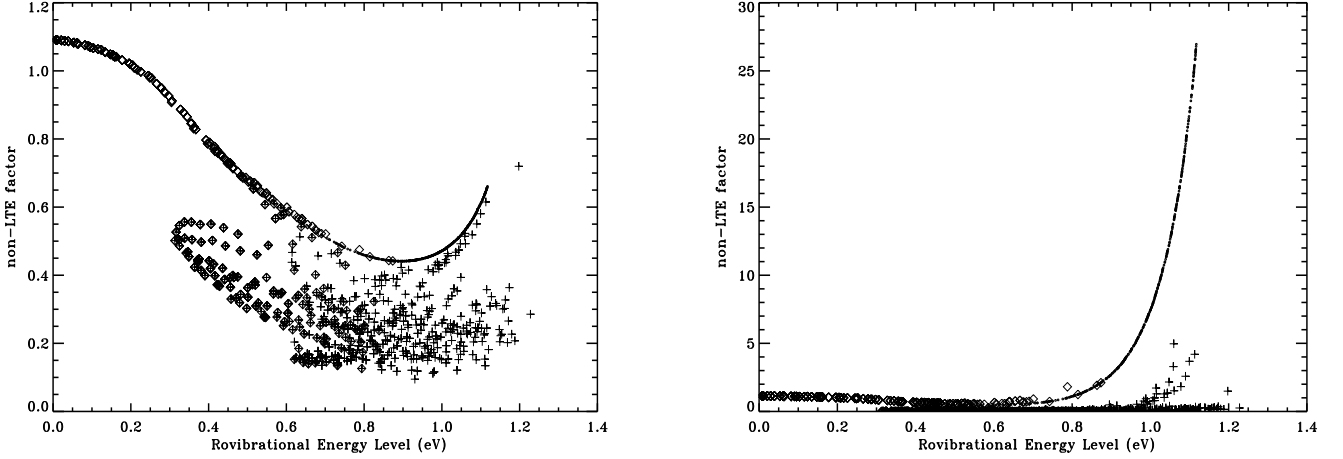


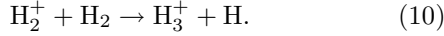
**Fig. 2.**— (a) Non-LTE factors ( $b_i$ ) for 1012 rovibrational levels computed using the line list of LM2001, for a collision frequency with  $\text{H}_2$  of  $n(\text{H}_2)k_c = 100 \text{ sec}^{-1}$ . Diamond and plus signs are for lower and upper level of radiative transitions, respectively, triangles are for levels with no radiative transitions. (b) Same as (a), but for a collision frequency of  $n(\text{H}_2)k_c = 1 \text{ sec}^{-1}$ .

levels that can be accessed by de-excitation. Oka & Epp (2004) suggested another way of estimating the de-excitation coefficients using a rather ad hoc method, in which the sum of their de-excitation coefficients from a given level increases with the number of levels below it. In the absence of other laboratory or theoretical calculations, these two ways of estimating the de-excitation coefficients should be considered as a source of uncertainty in the population models.

The production of a rovibrational level of  $\text{H}_3^+$ ,  $i$ , can be expressed as follows:

$$P_i = R_i + n(\text{H}_2) \left( \sum_{j < i} n_j k_{ji} + \sum_{k > i} n_k k_{ki} \right) + \sum_{k > i} n_k A_{ki}, \quad (9)$$

where  $R_i$  is the rate of chemical production of  $\text{H}_3^+$  from the reaction



The first and second summations represent the rates of collisional excitation from a lower level  $j$  to upper levels  $i$ , and collisional deexcitation from upper levels  $k$  to a lower level  $i$ , respectively. The third summation represents the radiative decay from upper levels  $k$  to a lower level  $i$ . The number density of the  $i$ -th level,  $n_i$ , is sometimes replaced by a non-LTE factor  $b_i$ , which is defined by the relationship

$$n_i \equiv b_i g_i \exp(-E_i/kT). \quad (11)$$

with  $i$  starting from 1. The ground state  $i = 0$  is a non-physical state, it only gives reference to the energy levels. In other words, the ground state is not populated at all. If LTE prevails, the non-LTE factor  $b_i$  is equal to unity for all the levels. The absolute value of

$R_i$  determines the total number density of  $\text{H}_3^+$ , which is the summation of  $n_i$  starting from  $i = 1$ .

The loss of a rovibrational level  $i$  can be expressed as

$$L_i = n_i n_e \alpha_e + n_i \sum_{j > i} A_{ji} + n(\text{H}_2) \times \left( \sum_{j < i} n_j k_{ij} + \sum_{k > i} n_k k_{ik} \right). \quad (12)$$

The first term on the right represents the loss by dissociative recombination, which can be expressed as



where  $n_e$  and  $\alpha_e$  are the electron density and dissociative recombination coefficient of  $\text{H}_3^+$ , respectively. Since no information is available on the dissociative recombination coefficients for individual  $\text{H}_3^+$  levels,  $\alpha_e$  is here assumed to be equal to  $3 \times 10^{-8} \text{ cm}^3 \text{ s}^{-1}$  for all the rovibrational levels. Johnsen and Guberman (2010) recently reviewed the laboratory and theoretical studies on recombination, reporting  $7 \times 10^{-8} \text{ cm}^3 \text{ s}^{-1}$  at an electron temperature of 300 K, and  $-1.3 \times 10^{-8} + 1.27 \times 10^{-6} T_e^{-0.48}$ . Measured  $\text{H}_3^+$  recombination coefficients were somewhat controversial, being in the range of  $10^{-7} - 10^{-9} \text{ cm}^3 \text{ s}^{-1}$  over the last four decades (see for example Leu et al. 1973; Adams et al. 1984; Plasil et al. 2002), but now a consensus seems to be reached after Johnsen and Guberman (2010)'s work. The exact value of the coefficient used in the model affects the total density of  $\text{H}_3^+$ , not the relative populations of rovibrational levels.

The first summation term on the right side of Eq. 12 represents the radiative decay from all upper states  $j$  to the lower state  $i$ . The second and third summations represent the collisional de-excitation from a level  $i$  to

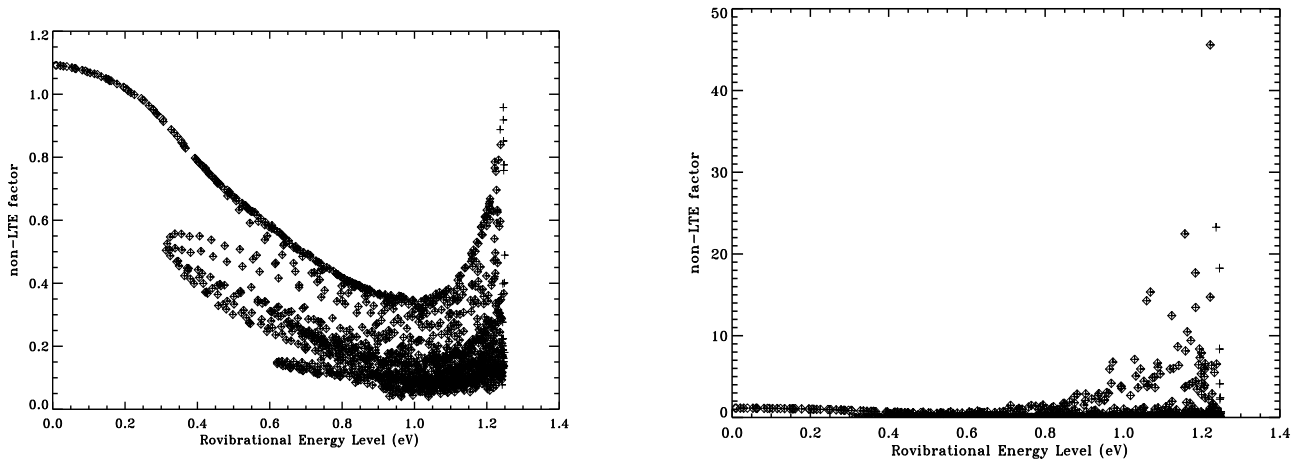


**Fig. 3.**— (a) Non-LTE factors ( $b_i$ ) for the 1405 rovibrational levels computed using the line list of UCL1996 for a collision frequency with  $\text{H}_2$  of  $n(\text{H}_2)k_c = 100 \text{ sec}^{-1}$ . Diamond and plus signs are for lower and upper levels of radiative transitions, respectively. (b) Same as (a), except for a collision frequency of  $n(\text{H}_2)k_c = 1 \text{ sec}^{-1}$ .

lower levels  $j$  with rate coefficients  $k_{ij}$ , and the collisional excitations from a state  $i$  to upper levels  $k$  with rate coefficients  $k_{ik}$ , respectively.  $\text{H}_3^+$  ions produced by the reaction Eq. 10 survive for a lifetime of  $1/(n_e\alpha_e)$  until they are neutralized by dissociative recombination. The lifetime of  $\text{H}_3^+$  is typically about 100 sec near the  $\text{H}_3^+$  density peak in the Jovian ionosphere, and is much longer at higher altitudes. We assume an  $\text{H}_3^+$  lifetime of 100 sec in the calculations, but its exact value does not affect the relative populations of levels.

Under steady state conditions, the number densities  $n_i$  or the non-LTE factors  $b_i$  can be derived by equating the production and loss rates (i.e.,  $P_i = L_i$ ), which establishes a system of linear equations. This set of equations can be solved using a standard matrix inversion method, since the coefficient matrix for the linear equations behaves well for the ambient  $\text{H}_2$  densities and temperatures relevant to the Jovian ionospheres. Conceptually, the number density of level  $i$  can be expressed as

$$n_i = \frac{R_i + RP_i + n(\text{H}_2)CP_i}{n_e\alpha_e + RL_i + n(\text{H}_2)CL_i}, \quad (14)$$

where  $RP_i$  is the sum of all the radiative production rates,  $CP_i$  is the sum of the collisional production rates from all upper levels included to level  $i$ ,  $RL_i$  is the specific radiative loss rate (or the inverse radiative decay time  $\tau_r^{-1}$ ), and  $CL_i$  is the sum of collisional transition rate coefficients from level  $i$  to all the levels included. In the limit of large  $\text{H}_2$  densities, where collisional processes dominate over radiative and chemical processes, LTE prevails and all the number densities  $n_i$  are equal to their LTE values; thus, the non-LTE coefficients  $b_i$  are unity. In the low  $\text{H}_2$  density limit, collisional production and loss, and radiative production all become negligible, making the chemical production and radiative decay dominant; the population  $n_i$  is then approx-

imately the chemical production rates  $R_i$  divided by the specific radiative decay rate  $RL_i$ . The chemical production from the reaction of  $\text{H}_2^+$  with  $\text{H}_2$  may vary among the rovibrational levels. We assume that  $R_i$  is proportional to the statistical weight of level  $i$ , namely  $(2J+1) \times (2S+1)$ , where  $J$  and  $S$  are the rotational quantum number and the nuclear spin number, respectively. This assumption mainly affects the populations of high rovibrational levels at very low ambient densities.

In the first model, Eqs. 9 and 12 were solved for 1012 rovibrational levels with energies up to  $10000 \text{ cm}^{-1}$  by including all the combinations of collisional transitions between these levels, and 823 radiative transitions from the LM2001 list. In the alternative model, the rate equations were solved for 1405 rovibrational levels with the 69528 radiative transitions in the UCL1996 line list.

#### 4. RESULTS AND DISCUSSION

The non-LTE factors of the rovibrational levels are calculated for seven different  $\text{H}_2$  densities:  $5 \times 10^{13}$ ,  $5 \times 10^{12}$ ,  $5 \times 10^{11}$ ,  $5 \times 10^{10}$ ,  $5 \times 10^9$ ,  $5 \times 10^8$  and  $5 \times 10^7$ , which correspond to collision frequencies of  $10^5$ ,  $10^4$ ,  $10^3$ ,  $10^2$ ,  $10$ ,  $1$  and  $0.1 \text{ sec}^{-1}$ , respectively, and to altitudes of about 300, 400, 600, 900, 1400, 1800, 2200 km in the Jovian auroral thermosphere, respectively (Grodent et al. 2001; Melin et al. 2005). The temperatures of 900, 1000, 1100, 1200, 1300 and 1400 K were used as representative of the conditions in the Jovian auroral regions.

Figs. 2a and 2b show the model non-LTE factors for 1012 levels for the cases of collision frequencies of 100 and  $1 \text{ sec}^{-1}$ , respectively, using the 823 radiative transitions in the LM2001 line list for an ambient temperature of 1000 K. In the figures, the rovibrational levels connected to one or more lower levels in radiative

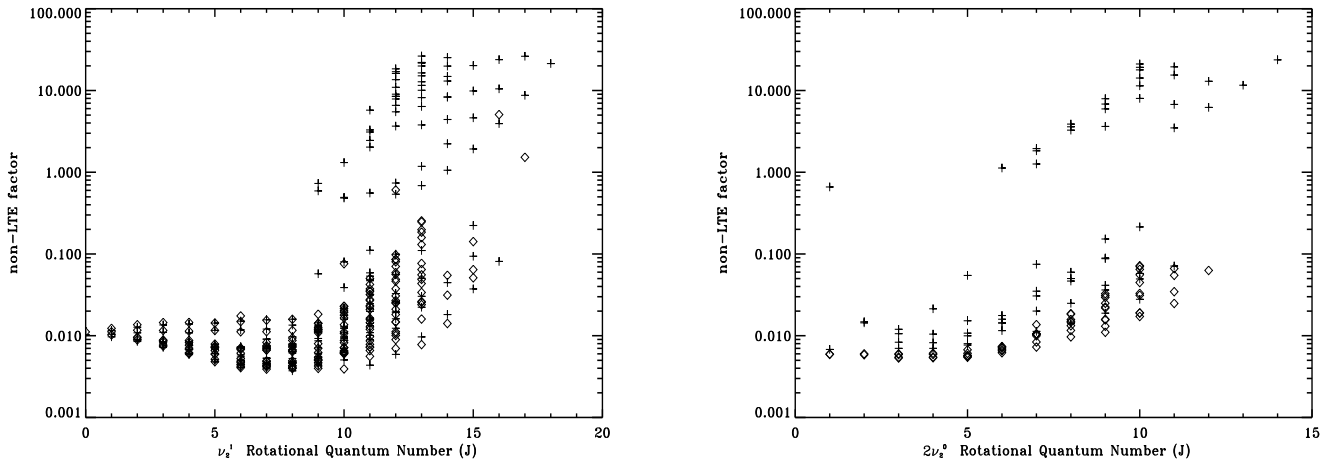


**Fig. 4.**— (a) Non-LTE factors  $b_i$  for rotational levels in the  $\nu_2^1$  vibrational state. Plus and diamond signs represent the results using the LM2001 and the UCL1996 line lists, respectively. The calculations assume collision frequencies with  $\text{H}_2$  of  $n(\text{H}_2)k_c = 1 \text{ sec}^{-1}$  and  $T = 1000 \text{ K}$ . (b) Same as (a), except for the  $2\nu_2^0$  vibrational state.

transitions are shown with diamond signs and those connected to upper levels in radiative transitions are denoted with plus signs. Levels not connected by any radiative transitions are indicated with a small circle. There are 414 non-radiating levels, 489 upper levels that radiate to one or more lower levels, 258 lower levels to which one or more of the upper levels radiate, and 149 levels that act as both upper and lower levels of the radiative transitions. Most of the non-LTE factors for  $\text{H}_2$  densities of  $\sim 5 \times 10^{10} \text{ cm}^{-3}$  are significantly less than unity, as shown in Fig. 2a. However, those for  $\text{H}_2$  densities of  $5 \times 10^8 \text{ cm}^{-3}$  show more prominent deviations from unity, as shown in Fig. 2b. At collision frequencies greater than about  $10^4 \text{ sec}^{-1}$ , or at  $\text{H}_2$  densities greater than about  $5 \times 10^{12} \text{ cm}^{-3}$ , the non-LTE factors for almost all the levels approach unity, indicating that LTE prevails.

In Fig. 2a, the upper levels of radiative transitions (plus sign) show significant depletions due to radiative decay ( $b_i \ll 1$ ), whereas those levels that do not decay radiatively are less depleted; levels lower than 0.2 eV are even overpopulated, due to production by radiative decay from upper levels. Non-LTE effects are more prominent in Fig. 2b than in Fig. 2a, since the rovibrational levels are less frequently interchanged by collisions due to smaller  $\text{H}_2$  densities. The non-radiative levels maintain the assumed nascent distribution produced from the chemical reaction of  $\text{H}_2^+$  with  $\text{H}_2$ . At collision frequencies less than about  $1 \text{ sec}^{-1}$ , or at  $\text{H}_2$  densities less than  $5 \times 10^8 \text{ cm}^{-3}$ , the lack of information on the nascent distributions reduces the certainty of the computed populations of the high  $\text{H}_3^+$  levels, whose nascent distribution may differ drastically from the Boltzmann distribution.

The non-LTE factors, shown in Figs. 3a and 3b, are the results of the alternative model, in which the 69619 radiative transitions in the UCL1996 line list

were adopted. The conditions used to obtain the results in Figs. 3a and 3b are the same as those in Figs. 2a and 2b, respectively. Although all of the 1405 rovibrational levels in this model are connected by one or more radiative transitions, the overall distributions of the non-LTE factors are very similar to those computed with the LM2001 line list. This indicates that the LM2001 line list includes most of the important transitions. However, some of the rovibrational levels, especially the high  $J$  levels exhibit significant differences in the non-LTE regime from the model which uses the LM2001 line list.

In Figs. 4a and 4b, the non-LTE factors of the levels in the  $\nu_2^1$  and  $2\nu_2^0$  states are displayed as a function of the rotational quantum number  $J$ , respectively. The overall distributions of non-LTE factors computed with the LM2001 list are more widely scattered, especially at high  $J$  numbers, than those obtained with the UCL1996 line list. The difference in the two models is most visible in the distributions of the  $J$  levels in the  $2\nu_2^0$  state, as shown in Fig. 4b. The widely scattered distributions appear to originate from incomplete radiative relaxation of the levels involved, probably due to deficiencies in the LM2001 line list, and indicate large uncertainties in the rotational temperatures derived from ratios of the rotational level populations in a given vibrational state.

Although the non-LTE factors shown in Figs. 4a and 4b are mostly much less than unity, the rotational temperatures may not be significantly different from ambient temperatures. In observational studies of the Jovian ionosphere, investigators often assume that the rotational temperatures of  $\text{H}_3^+$  may represent the thermospheric temperatures at the  $\text{H}_3^+$  emission altitude. This assumption may be valid if the non-LTE factors of different  $J$  levels are equal, indicating that non-LTE effects deplete the rotational levels to the same extent.

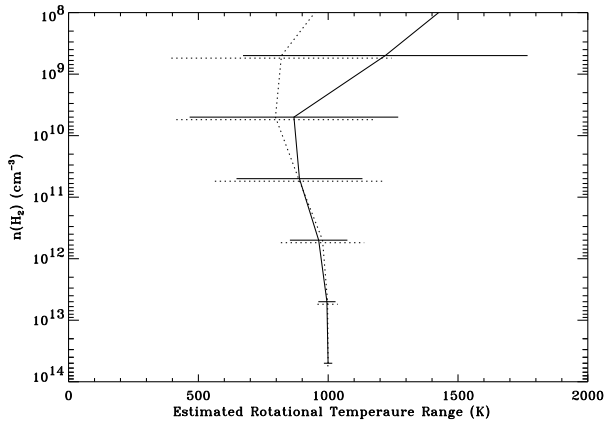


**Fig. 5.**— Estimated mean rotational temperatures from pairs of rotational levels in the  $\nu_2^1$  state (solid curve), and in the  $2\nu_2^0$  state (dotted curve). The rovibrational population model was computed with the UCL1996 radiative transition list. The horizontal bars indicate the standard deviations from the mean rotational temperatures.

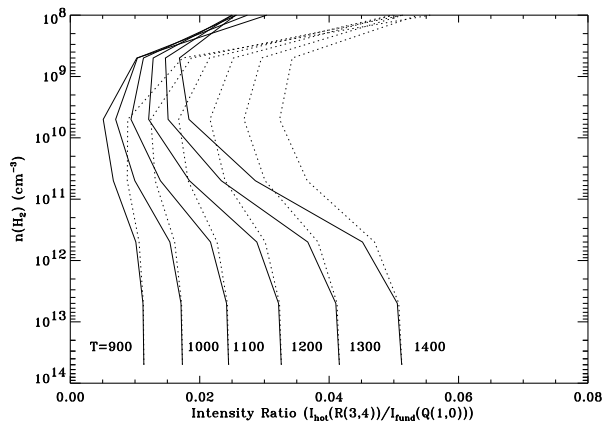


**Fig. 6.**— Intensity ratios of the line R(3,4) in the hot band to the line Q(1,0) in the fundamental band, as a function of ambient  $\text{H}_2$  densities, for various thermospheric temperatures. The solid curves are computed using the 69528 transitions from the UCL1996 line list. The dotted curves are computed using the LM2001 line list. Note that the solid and dotted curves in the non-LTE regime differ significantly from each other, and from those in the simple three-level model illustrated in Fig. 1.

This situation is sometimes called “quasi-LTE”. We have investigated the quasi-LTE assumption, by deriving rotational temperatures from all the pairs of rotational levels in the  $\nu_2^1$  and  $2\nu_2^0$  states.

In Fig. 5, we show the computed mean values and standard deviations of the derived rotational temperatures for the thermospheric  $\text{H}_2$  densities from  $10^8$  to  $10^{14}$   $\text{cm}^{-3}$ . The solid and dotted curves represent the mean rotational temperatures of the  $\nu_2^1$  and  $2\nu_2^0$  states, respectively, and the solid and dotted bars indicate the corresponding standard deviations from the mean values. For this calculation, we use the UCL1996 tran-

sition list. The standard deviations indicate the uncertainty of the derived rotational temperatures from each set of pairs of levels. At high altitudes in the thermosphere, as the ambient  $\text{H}_2$  density decreases, the rotational temperatures become more uncertain, but the mean rotational temperatures of the  $\nu_2^1$  state are significantly larger than the assumed ambient thermal temperature of 1000 K. This effect is due to the relatively large populations of high  $J$  levels, as shown in Fig. 4a. By excluding high  $J$  levels, one may reduce this deviation when deriving rotational temperatures. Standard deviations of  $\nu_2^1$  and  $2\nu_2^0$  rotational temperatures become quite significant, as large as  $\pm 220$  K and  $\pm 360$  K, respectively, at an  $\text{H}_2$  density of  $5 \times 10^{10}$   $\text{cm}^{-3}$ . This shows that rotational temperatures derived from observations of Jovian  $\text{H}_3^+$  emissions in the fundamental and overtone bands are not good indicators of the ambient thermospheric temperatures, since a considerable contribution to the Jovian  $\text{H}_3^+$  emissions originates from altitudes in the non-LTE region. Therefore, one must be careful in interpreting the rotational temperatures derived from a small number of line intensities, especially in the overtone and hot bands. In particular, attempts to derive thermospheric temperatures from ratios of lines in the hot and fundamental bands may not give correct results at high altitudes, where ambient  $\text{H}_2$  densities are low.

As an example, in Fig. 6 we have computed the intensity ratio of the R(3,4) line in the hot band to that of the Q(1,0) line in the fundamental band, using the two rovibrational population models. The solid and dotted curves were calculated using the UCL1996 and LM2001 line lists, respectively. It is evident that non-LTE effects become significant at an  $\text{H}_2$  density less than  $10^{12}$   $\text{cm}^{-3}$ , which is similar to the result of the simple three-level model shown in Fig. 1. Thus, the relative populations of the upper levels, namely  $J' = 4$  in the  $2\nu_2^0$  and  $J' = 1$  in the  $\nu_2^1$  vibrational levels, maintain LTE values up to  $\text{H}_2$  densities of  $10^{12}$   $\text{cm}^{-3}$  despite their large Einstein A values of 66 and 129  $\text{sec}^{-1}$ , respectively. In the simple three-level model, a collision frequency greater than about 100  $\text{sec}^{-1}$  is required to maintain LTE, because the radiative decay of the levels characterized by transition probabilities of about 100  $\text{sec}^{-1}$  is fast. The inclusion of a large number of levels appears to yield similar results, since the total collisional loss rate from a level is approximately the same – regardless of the number of levels included.

The intensity ratios in Fig. 6 decrease with the  $\text{H}_2$  density range of  $10^{13}$  -  $10^{10}$   $\text{cm}^{-3}$ , opposite to those of the simple three-level model shown in Fig. 1. This is because the collisional rate coefficients used in the comprehensive models differ from those used in the three-level model, in which a constant value is assumed for the de-excitation coefficients  $k_{20}$  and  $k_{10}$ . The de-excitation coefficients used in the comprehensive models are smaller for high levels than for low levels, because the total de-excitation rate to all the lower levels is normalized to be the Langevin value. The collisional

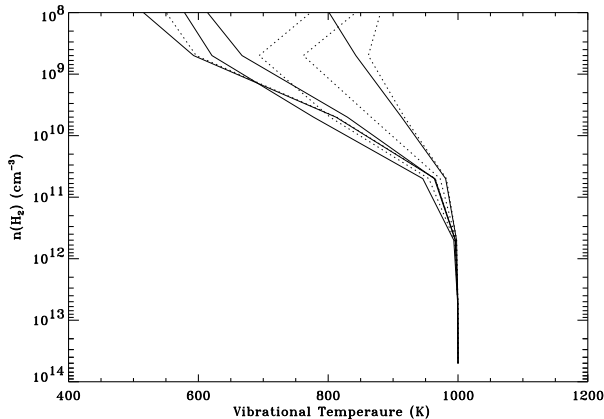


**Fig. 7.**— Vibrational temperatures of  $\nu_2^1$ ,  $2\nu_2^2$ ,  $2\nu_2^0$  and  $\nu_1$  states vs. ambient  $\text{H}_2$  densities, sorted from largest to smallest departures from the assumed temperature of 1000 K. The solid and dotted lines were computed with the UCL1996 and LM2001 line lists, respectively.

excitation coefficient from the ground level to the upper level of the hot band line (in  $2\nu_2$  state) is smaller than that for the fundamental band line (in  $\nu_2$  state), because of the larger energy difference, and thus the hot band levels in these models are less collisionally excited than in the three-level model. As the ambient  $\text{H}_2$  density decreases, radiative decay becomes dominant over collisional de-excitation as a loss process, but collisional excitation from the ground level (whose population is the largest) is still the major production process. Thus, the population ratio of the upper to the lower level decreases as the ambient  $\text{H}_2$  density decreases, until the direct chemical reaction ( $CP_i$ ) and radiative production from higher levels ( $RP_i$ ) dominate the production process; see Eq. 14.

For  $\text{H}_2$  densities less than  $10^{10} \text{ cm}^{-3}$ , the chemical production rate is important. Since it is assumed to be proportional to the statistical weight of the rovibrational levels, the ratio of production rates for R(3,4) to Q(1,0) is  $(2 \times 4 + 1) \times 2 / (2 \times 1 + 1) \times 4 = 1.5$ , leading to an increase in the intensity ratios. The production rate due to radiation from higher levels to these two levels depends on the number of radiative transitions used in the model. The model with the UCL1996 list (solid lines in Fig. 6) shows less increase in the intensity ratios than the model with the LM2001 list. This is because the rotational levels in the  $\nu_2^1$  state, which are the source of the Q(1,0) line, are significantly enhanced by radiative transitions from the upper levels, most of which were not included in the LM2001 line list. More specifically, the radiative production of the J=1 level in  $\nu_2$  state is larger than the J=4 level in  $2\nu_2$  state in the model with the UCL1996 list, thereby reducing the increase in the intensity ratios due to chemical production, which depends on the statistical weight ratio of these levels. In the model with LM2001, on other hand, the radiative productions for these two levels are neg-

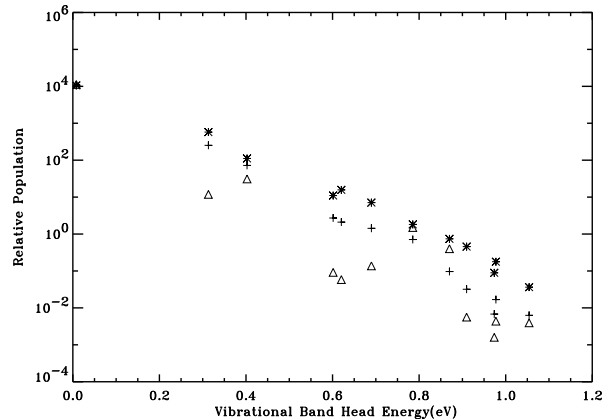


**Fig. 8.**— Relative populations of the vibrational states for collision frequencies  $n(\text{H}_2)k_c$  equal to  $1 \text{ sec}^{-1}$  (triangle),  $100 \text{ sec}^{-1}$  (plus),  $10^4 \text{ sec}^{-1}$  (asterisk). The asterisk signs represent the LTE population. The vibrational band populations do not differ significantly from LTE for collision frequencies of  $\geq 10^3 \text{ sec}^{-1}$ . The vibrational states are  $\nu_2^1$ ,  $\nu_1$ ,  $2\nu_2^0$ ,  $2\nu_2^2$ ,  $\nu_1 + \nu_2^1$ ,  $2\nu_1$ ,  $3\nu_2^1$ ,  $3\nu_2^3$ ,  $\nu_1 + 2\nu_2^0$ ,  $\nu_1 + 2\nu_2^2$  and  $2\nu_1 + \nu_2^1$ , sorted by increasing energies.

ligible compared with the chemical production at very low  $\text{H}_2$  densities, thus resulting in a larger increase in the intensity ratios than the model with UCL1996. The differences between the intensity ratios in the two models are indicative of the uncertainties that affect the derivation of thermospheric temperatures in the non-LTE region.

In Fig. 7, the vibrational temperatures  $T_v$  derived from the  $\nu_2^1$ ,  $\nu_1$ ,  $2\nu_2^0$  and  $2\nu_2^2$  states are shown for a kinetic temperature of 1000 K, as a function of ambient  $\text{H}_2$  densities, over the range  $10^{14} - 10^8 \text{ cm}^{-3}$ . The vibrational temperature  $T_v$  is defined for a given kinetic temperature  $T$  by the relationship:

$$n_v/n_v^* = \exp(-E_v/kT_v) / \exp(-E_v/kT) \quad (15)$$

where  $n_v$  and  $n_v^*$  are the number densities of the vibrational states for the non-LTE and LTE cases, respectively, and  $E_v$  is the energy of the band head of the vibrational state. The number densities of the vibrational states are the sums of the number densities of the individual rovibrational states. Results for the models computed using both the LM2001 and UCL1996 line lists are shown. The vibrational temperatures begin to depart from kinetic temperatures at an  $\text{H}_2$  density of about  $10^{11} \text{ cm}^{-3}$ , in good agreement with the vibrational population model of Melin et al (2005).

In Fig. 8, the populations of the vibrational states for the UCL1996 model are presented as a function of band head energies  $E_v$ , for  $\text{H}_2$  collision frequencies of  $10^4$ ,  $10^2$  and  $1 \text{ sec}^{-1}$ . The vibrational states, in increasing order of energies, are  $\nu_2^1$ ,  $\nu_1$ ,  $2\nu_2^0$ ,  $2\nu_2^2$ ,  $\nu_1 + \nu_2^1$ ,  $2\nu_1$ ,  $3\nu_2^1$ ,  $3\nu_2^3$ ,  $\nu_1 + 2\nu_2^0$ ,  $\nu_1 + 2\nu_2^2$  and  $2\nu_1 + \nu_2^1$ . The relative populations at collision frequencies less than  $10^4 \text{ sec}^{-1}$  clearly show depletions from the LTE values, due to ra-

diative decay. For the model with the LM2001 list (not shown), the high vibrational states are overpopulated compared to the LTE values, due to incomplete radiative decay of the assumed nascent populations. The overall distribution of vibrational populations shown in Fig. 8 is similar to that of the model presented by Kim et al. (1992), which includes only vibrational states. A small difference is visible, because Kim et al. (1992) included V-V energy transfer from  $\text{H}_2(v > 0)$  to  $\text{H}_3^+$ .

In the models presented here, we ignore interactions of  $\text{H}_3^+$  rovibrational levels with other constituents such as H atoms, and vibration energy transfer reactions with  $\text{H}_2(v \geq 1)$ . Collisions with H atoms and vibrational energy transfer from  $\text{H}_2(v \geq 1)$  may play significant roles in reducing the non-LTE effects of  $\text{H}_3^+$  emission in the Jovian ionosphere at high altitudes. The Jovian thermosphere temperature is higher above the peak of the  $\text{H}_3^+$  density profile near 600 km (Kim et al., 2001). The fraction of  $\text{H}_3^+$  emission from high altitudes could increase rapidly if non-LTE effects are reduced, as noted by Melin et al (2005). There are some remaining uncertainties both in the collisional rate coefficients and in the radiative transition probabilities between the rovibrational levels, and thus the process of retrieving temperatures and column densities of  $\text{H}_3^+$  is significantly model-dependent.

The referee raised a concern that collisions with electrons in the topside Jovian ionosphere may be more dominant in rotational excitation and de-excitation rates than with  $\text{H}_2$ , referring to Dickinson et al. (1977) which suggested that electrons are  $10^5$  times more efficient to excite HCN rotation levels than molecular hydrogens in the cold interstellar clouds. However, (de)excitation processes of  $\text{H}_3^+$  proceed via an intermediate through a chemical reaction (8), which is categorically different from those of HCN. Kokouline et al. (2010) calculated rate constants of  $10^{-7}$  and  $10^{-9}$   $\text{cm}^3\text{s}^{-1}$  at  $T = 1000$  K for rotational and vibrational de-excitation of  $\text{H}_3^+$  by electron impact, respectively, while Oka & Epp (2004) estimated  $2 \times 10^{-9}$   $\text{cm}^3\text{s}^{-1}$  for total rotational de-excitation by  $\text{H}_2$  through reaction (8), as used in this model. Since the Jovian ionosphere typically shows electron densities of  $10^4$   $\text{cm}^{-3}$  at an altitude that corresponds to the lowest  $\text{H}_2$  density of  $10^8$   $\text{cm}^{-3}$  considered in the model, the electron collision cannot be more dominant for (de)excitation of  $\text{H}_3^+$  rovibrational levels than  $\text{H}_2$ . A more realistic model, however, should include collisions of H atoms as well as electrons.

## 5. CONCLUSIONS

We have investigated the effects of non-LTE on the  $\text{H}_3^+$  level populations in order to interpret observations of the 2 and 3.5 micron  $\text{H}_3^+$  emissions from the Jovian ionosphere. We first considered a simple three-level model to estimate these effects on the intensity ratio of the R(3,4) line in the hot band to the Q(1,0) line in

the fundamental band, which have been observed from the Jovian auroral regions. This model, unlike a similar model published previously, shows only marginal changes in the ratio due to non-LTE effects at ambient  $\text{H}_2$  densities of  $10^{12}$   $\text{cm}^{-3}$  or less. We then constructed more comprehensive models for the populations of the rovibrational levels by including all the collisional and radiative transitions between the  $\text{H}_3^+$  rovibrational levels with energies less than  $10000$   $\text{cm}^{-1}$ , using the line lists compiled by LM2001 and UCL1996. In these models, non-LTE effects appear at about the same ambient  $\text{H}_2$  densities as in the three-level model. The intensity ratios of the lines in the hot and fundamental bands are dramatically influenced by non-LTE effects, depending on the collisional and radiative transitions used in the model. The model also shows that rotational temperatures derived from lines in the  $\nu_2$  and  $2\nu_2$  bands, which have been thought to be close to the ambient temperature, may differ significantly from the kinetic temperatures in the non-LTE regime. We conclude that extracting thermospheric neutral temperatures from the observed  $\text{H}_3^+$  infrared line ratios is highly model dependent. The present investigation may be useful to indicate the ambient  $\text{H}_2$  number density at which the rotational levels begin to be dominated by non-LTE effects.

## ACKNOWLEDGMENTS

This study was financially supported by a research grant from Chungnam National University in 2010.

## REFERENCES

- Adams, N. G., Smith, D., & Alge, E. J. 1984, Measurements of Dissociative Recombination Coefficients of  $\text{H}_3^+$ (+),  $\text{HCO}^+$ (+),  $\text{N}_2\text{H}^+$ (+) and  $\text{CH}_5^+$ (+) at 95 and 300K Using the FALP Apparatus, *Chem. Phys.*, 81, 1778
- Dickinson, A. S., Phillips, T. G., Goldsmith, P. F., Percival, L. C., & Richards, D. 1977, Rotational Excitation of Molecules by Electrons in Interstellar Clouds, *A&A*, 54, 645
- Drossart, P., & 11 Colleagues. 1989, Detection of  $\text{H}_3^+$  on Jupiter, *Nature*, 340, 539
- Grodent, D., Waite, Jr. J. H., & Gerard, J.-C. 2001, A Self-Consistent Model of the Jovian Auroral Thermal Structure, *J. Geophys. Res.*, 106, 12933
- Johnsen, R., & Guberman, S. L. 2010, Chapter 3. Dissociative Recombination of  $\text{H}_3^+$  Ions with Electrons: Theory and Experiment, *Advances in Atomic, Molecular, and Optical Physics*, 59, 75
- Kim, Y. H., Fox, J. L., & Porter, H. S. 1992, Densities and Vibrational Distribution of  $\text{H}_3^+$  in the Jovian Auroral Ionosphere, *J. Geophys. Res.*, 97, 6093
- Kim, Y. H., Pesnell, W. D., Grebowsky, J. M., & Fox, J. L. 2001, Meteoric Ions in the Ionosphere of Jupiter, *Icarus*, 150, 261
- Kokouline, V., Faure, A., & Tennyson, J. 2010, Calculation of Rate Constants for Vibrational and Rotational

- Excitation of the  $\text{H}_3^+$  Ion by Electron Impact, *MNRAS*, 405, 1195
- Kreckel, H., & 22 Co-Authors. 2005, High-Resolution Dissociative Recombination of Cold  $\text{H}_3^+$  and First Evidence for Nuclear Spin Effects, *PRL*, 95, 263201
- Lam, H. A., Achilleos, N., Miller, S., Tennyson, J., Trafton, L. M., Geballe, T. R., & Ballester, G. E. 1997, A Baseline Spectroscopic Study of the Infrared Auroras of Jupiter, *Icarus*, 127, 379
- Leu, M. T., Biondi, M. A., & Johnsen, R. 1973, Measurements of Recombination of Electrons with  $\text{H}_3^+$  and  $\text{H}_5^+$  Ions, *Phys. Rev. A*, 8, 413
- Lindsay, C. M., & McCall, B. J. 2001, Comprehensive Evaluation and Compilation of  $\text{H}_3^+$  Spectroscopy, *J. Mol. Spec.*, 219, 60
- Maillard, J.-P., Drossart, P., Watson, J. K. G., Kim, S. J., & Caldwell, J. 1990,  $\text{H}_3^+$  Fundamental Band in Jupiter's Auroral Zones at High Resolution from 2400 to 2600 Inverse Centimeters, *ApJ*, 363, 37
- Melin, H., Miller, S., Stallard, T., & Grodent, D. 2005, Non-LTE Effects on  $\text{H}_3^+$  Emission in the Jovian Upper Atmosphere, *Icarus*, 178, 97
- Miller, S., Achilleos, N., Ballester, G. E., Lam, H., Tennyson, J., Geballe, T. R., & Trafton, L. M. 1997, Mid-To-Low Latitudes  $\text{H}_3^+$  Emission from Jupiter, *Icarus*, 130, 57
- Neale, L., Miller, S., & Tennyson, J. 1996, Spectroscopic Properties of the  $\text{H}_3^+$  Molecule: a New Calculated Line List, *ApJ*, 464, 516
- Oka, T., & Epp, E. 2004, The Nonthermal Rotational Distribution of  $\text{H}_3^+$ , *ApJ*, 613, 349
- Perry, J. J., Kim, Y. H., & Fox, J. L. 1999, Chemistry of the Jovian Auroral Ionosphere, *Journ. Geophys. Res.*, 104, 16, 541
- Plasil, R., Glosik, J., Poterya, V., Kudrna, P., Rusz, J., & Tichy, M. 2002, Advanced Integrated Stationary Afterglow Method for Experimental Study of Recombination of Processes of  $\text{H}_3^+$  and  $\text{D}_3^+$  Ions with Electrons, *Int. J. Mass Spect.*, 218, 105
- Raynaud, E., Lellouch, E., Maillard, J.-P., Gladstone, G. R., Waite, Jr. J. H., Bezard, B., Drossart, P., & Fouchet, T. 2004, Spectro-Imaging Observations of Jupiter's 2 Micron Auroral Emission. I.  $\text{H}_3^+$  Distribution and Temperature, *Icarus*, 171, 133
- Stallard, T., Miller, S., Millward, G., & Joseph, R. D. 2002, On the Dynamics of the Jovian Ionosphere and Thermosphere II. The Measurement of  $\text{H}_3^+$  Vibrational Temperature, Column Density, and Total Emission, *Icarus*, 156, 498